CHAPTER 1

Introduction

In this chapter we introduce the basic concepts used in this thesis. We give a brief overview of structure formation theory, stressing the importance of baryonic physics. Chemical evolution models - beginning with simple analytic but moving on to numeric models - are described and their strengths and weaknesses discussed. Having established a context, the contents of this thesis are outlined, briefly describing the contents and findings of each chapter. We conclude by considering the outlook for the field.

For over one hundred years now astronomers have been able to study the universe on the largest scales. Recently, this field has become particularly exciting as we have entered an era of 'precision cosmology'. Due in large part to the very detailed mapping of the sky in the microwave band (e.g., *COBE*[1], *WMAP*[2]) and wide field extragalactic surveys such as the *Sloan Digital Sky Survey (SDSS)*[3], a solid understanding of large scale structure in the universe can be obtained. On the other hand, sophisticated computer simulations of the universe such as the *Millennium Simulation*[4] have yielded a number of clues as to how this structure formed. Both of these aspects of research in this area have benefited greatly from recent technological advancements that have only now made these projects possible.

These developments have been built upon a solid foundation of cosmological theory that emerged in the first half of the twentieth century. The starting point of this theory is the Cosmological Principle, which assumes that the Universe is homogeneous and isotropic. This principle appears to be true on the very largest scales.

Given the Cosmological Principle, Einstein's equations of General Relativity can be solved for a fluid with energy density ρc^2 and pressure p. This solution is typically written in the form of the Friedmann equations:

$$\ddot{a} + \frac{4}{3}\pi G\left(p + \frac{3\rho}{c^2}\right)a = 0, \tag{1.1}$$

$$\dot{a}^2 + Kc^2 - \frac{8}{3}\pi G\rho a^2 = 0, \tag{1.2}$$

where G is the gravitational constant, K is the curvature of space-time, and a is the expansion factor of the Universe (we have used a dot to indicate a derivative with respect to proper time). The expansion factor is a parameter that relates comoving distances to proper distances measured at the present day viz. $d_p = ad_c$. The expansion factor is also used to define the Hubble parameter: $H \equiv \dot{a}/a$.

Observations over the past decade have shown that the universe is remarkably close to, if not completely flat (e.g. Spergel et al. 2007). In this case, the equations simplify slightly as the curvature K is zero. The matter-energy density of the universe can then be written as:

$$\rho_m = \rho_{\rm crit} = \frac{3H^2}{8\pi G}. \tag{1.3}$$

One can then predict the growth of structures from primordial fluctuations in the linear regime (typically referred to as linear theory). Considering only gravity, a matter density perturbation in an expanding universe is governed by:

$$\ddot{\delta} + 2H\dot{\delta} - \frac{3}{2}\Omega H^2\delta = 0, \tag{1.4}$$

where δ is the magnitude of the density perturbation and Ω is the ratio of the density to the critical density of the universe. This formalism breaks down if δ is significant

[1]http://lambda.gsfc.nasa.gov/product/cobe/
[2]http://map.gsfc.nasa.gov/
[3]http://www.sdss.org/
[4]http://www.mpa-garching.mpg.de/galform/millennium/

compared to unity, at which point more sophisticated modelling is required, often in the form of computer simulations. Note that structures of interest to most astronomers (galaxies, clusters of galaxies, etc.) are highly non-linear.

As such models became more sophisticated, astronomers soon became aware that the budget of matter in the universe is dominated by some unseen form, called 'dark matter'. Although other explanations exist (e.g., Modified Newtonian Dynamics - MOND), dark matter provides a solution on a wide range of scales, accounting for structure formation as well as galactic rotation curves. Since dark matter is so dominant, much work has been done with exclusively dark matter simulations.

These simulations have been very instructive, describing the hierarchical nature of structure formation. In this picture, haloes are assembled via mergers of smaller haloes rather than a monolithic collapse. The resulting correlation functions and halo statistics from such simulations match well with the observed distribution of matter on large scales[5].

To gain further insight, we must however move beyond the collapse of matter into haloes by gravity. While dark matter is thought to feel only gravity, the baryons (which in most cases are visible) in the universe can interact using other forces as well and are what is directly observed by astronomers. These baryons collapse into galaxies hosted by dark matter haloes, a process that involves a great deal of physical processes, including but not limited to hydrodynamics, gas heating and cooling, star formation, radiative, mechanical, and chemical[6] feedback from stars, and feedback from active galactic nuclei (AGN). The task in interpreting extra-galactic observations beyond the large-scale distribution of matter then becomes increasingly complicated.

To first order, structure formation is a competition between gravitational collapse and kinetic energy. When considering the collapse of dark matter haloes, one can simply apply the virial theorem:

$$2K = -U, \tag{1.5}$$

where K and U represent the total kinetic and potential energy of the system respectively. A halo will then typically collapse to fulfill this condition.

Since a gas cloud contains pressure forces, this is not the only condition that dictates how baryonic structures form. Under solely adiabatic conditions, the increasing thermal velocity dispersion of a collapsing cloud will at some point halt its formation. By equating the free-fall timescale ($t_{\rm ff} \simeq 1/\sqrt{G\rho}$, where ρ is the mean density of the medium and G is the gravitational constant) and the sound crossing timescale ($t_{\rm sc} \simeq L/c_{\rm s}$, where L is the mean diameter of the cloud, and $c_{\rm s}$ is the sound speed of the medium) we can arrive at the Jeans length, $L_{\rm J}$:

$$L_{\rm J} \simeq \frac{c_{\rm s}}{\sqrt{G\rho}}. \tag{1.6}$$

[5]Note that such simulations predict the large scale distribution of the dark matter - the connection to observable, visible matter is made via a halo population model.

[6]Note that here and throughout this thesis, we have use the word 'chemical' somewhat loosely since we are referring to nucleosynthesis and redistribution of elements, ignoring almost entirely chemical reactions between atoms and molecules.

Given a spherical cloud, this can be converted into a mass:

$$M_{\rm J} \simeq \frac{c_{\rm S}^3}{G^{3/2}\rho^{1/2}}, \tag{1.7}$$

above which a concentration of matter can collapse under the forces of gravity or fragment and below which said concentration will reach equilibrium by either expanding or evaporating.

The energy that is used to support the system can be radiated away via cooling. In this way we introduce another timescale, the cooling time:

$$t_{\rm cool} \equiv \frac{T}{dT/dt} \propto \frac{\rho T}{\Lambda}, \tag{1.8}$$

where Λ is the radiative cooling rate per unit volume. We can then consider three regimes: The first is where $t_{\rm cool} > t_H$, the Hubble time, defined as $1/H$, or roughly the age of the universe. In this regime, objects stay at the Jeans mass and evolve neither in density or temperature. For $t_{\rm ff} < t_{\rm cool} < t_H$, the gas can adjust itself in reaction to the cooling. In this case, an object undergoes a steady, monolithic collapse on a timescale of $t_{\rm cool}$. Finally, when $t_{\rm cool} < t_{\rm ff} < t_H$, the gas cannot adjust itself and collapses on a free-fall timescale. Such a cloud can fragment to form substructures which themselves would be subject to their own timescales.

There are currently two approaches to the modelling of baryonic physics in galaxy formation. One is semi-analytical modelling, which typically employs existing dark matter simulations[7] and uses numerical prescriptions for the various physical processes occurring at a given time. Such prescriptions are often physically motivated, with the uncertainties quantified using free parameters. The entire model is then tuned to match observations of the local universe. This method has its advantages and has had many successes (e.g., Kauffmann et al. 1993; Somerville & Primack 1999; Croton et al. 2006) over the past two decades. There are two main disadvantages to this method however. One problem is that such models tend to involve many free parameters, making interpretation troublesome (is a given effect real, or could another arbitrary set of parameters reproduce it?). Perhaps more important is that semi-analytical models incorporate highly simplified aspects of the physics involved in galaxy formation. For instance, rather than modelling haloes as intersections in the cosmic web, these models assume that haloes are spherically symmetric. This often results in the absence of crucial processes, such as accretion of cold gas in the form of filaments.

Another way to model the physics of baryons is to perform hydrodynamical simulations. Unfortunately, introducing baryonic physics into fully numerical simulations is far from straightforward. One must always be conscious of possible resolution effects as well as the limitations of the implementation of a given physical recipe. It is often necessary to concede one's ability to directly resolve a process and to use a so-called 'sub-grid' recipe to simulate the effects of said process on a larger scale. For example, current cosmological simulations can at best resolve objects of gas mass $\sim 10^5\ {\rm M}_\odot$. The

[7] Although halo mass functions (e.g., Press-Schechter formalism) and Monte-Carlo merging are also sometimes employed.

formation of a star takes place on scales many orders of magnitude below that, say $\sim 1\ \mathrm{M}_{\odot}$. As a result of this discrepancy in scales, simulations must invoke some law that approximates star formation on galactic scales without introducing some bias.

These processes often feed back into other processes as well as into structure formation. Ionizing photons from star formation, for instance, can inhibit further structure formation by heating the surrounding gas, thereby changing the typical mass of a collapsed object (e.g., Shapiro et al. 1994; Gnedin & Hui 1998). Other forms of feedback include energy and chemical feedback from supernovae and stellar winds.

Chemical feedback plays a prominent role in astrophysical studies on a wide range of scales. Despite the fact that 'metals' (elements heavier than helium) have abundances more than an order of magnitude lower than hydrogen and helium, they can profoundly influence objects ranging from protostars to galaxy clusters. A large amount of work, both theoretical and observational has been done in order to investigate the causes and the effects of chemical feedback (see for example table 3.5). Metals can act as tracers for various processes, as well as enrich gas clouds and impact their cooling (Sutherland & Dopita 1993), which in turn determine the timescale on which structures can form.

Metal production occurs during a large part of the history of the universe. After the Big Bang produced trace amounts of lithium and other light elements, there was a gap until the first stars formed. From then on, stars, supernovae, and exotic events such as neutron star mergers contributed to the enrichment of the almost pristine hydrogen and helium mix in the Universe.

These metals can indicate how star formation occurred, and as such can yield clues to the assembly of galaxies and clusters, fundamental questions deeply important to our understanding of the universe. We must therefore understand how metals are created, transported and how various quantities can give us information about the state of the system.

1.1 'Simple' Models

1.1.1 Purely Analytical Calculations

The idea of studying the chemical evolution of the universe is by no means new. Once astronomers realised that heavy elements are produced in stars, they could use analytic formulations to account for the current metal distribution. This involves some assumptions about the star formation rate/efficiency as well as the yield of such stars, but can provide some insight as to the nature of the enriched gas. The following treatment draws on Binney & Merrifield (1998).

The Closed Box

First considered by Talbot & Arnett (1971), the closed box model considers a system where no gas enters or leaves the system, but is recycled for new stars to be born. As galaxies are known to generate super-winds and have gas accreted from filaments, it

serves only as a toy model when applied to them. Galaxy clusters however, retain a large fraction of their gas and are reasonably well approximated by such a model. Naturally, the Universe as a whole is a truly a closed box. On the other hand, in both of these instances the instantaneous mixing approximation is unlikely to be valid.

In addition to the assumption of a closed box, we also make two more assumptions: the instantaneous mixing approximation and the instantaneous recycling approximation. The former simply means that the gas is always well mixed, while the latter means that stars that pollute the ISM do so immediately (i.e., the stellar lifetimes are zero).

We begin by considering a mass of gas M_g, with metal mass M_Z such that the metallicity is:

$$Z_g = M_Z/M_g. \tag{1.9}$$

Our total stellar mass M_* increases by $\Delta' M_*$ in some time interval. Let us consider ΔM_*, the amount of mass converted into stars *that stays in stars*, that is after stellar mass loss has been accounted for. Since the metal mass that is ejected is some constant fraction of $\Delta' M_*$ and ΔM_* will also be some constant factor times $\Delta' M_*$, we may denote the amount of heavy elements ejected as $y\Delta M_*$ (i.e., proportional to the amount that stays in stars) and we call y the yield. Thus the change in the gas phase metal mass in some time interval is just the amount of metals locked up in stars in that interval subtracted from the metal mass ejected in that interval:

$$\Delta M_Z = y\Delta M_* - Z\Delta M_* = (y - Z_g)\Delta M_*. \tag{1.10}$$

What we usually want to know is the metallicity, which changes as:

$$\Delta Z_g = \Delta\left(\frac{M_Z}{M_g}\right) = \frac{\Delta M_Z}{M_g} - \frac{M_Z}{M_g^2}\Delta M_g = \frac{1}{M_g}\left(\Delta M_Z - Z_g \Delta M_g\right). \tag{1.11}$$

Since mass is approximately[8] conserved, $\Delta M_* = -\Delta M_g$ this works out to

$$\Delta Z_g = \frac{1}{M_g}\left(\Delta M_Z - Z_g\Delta M_g\right) = \frac{1}{M_g}\left(-(y - Z_g)\Delta M_g - Z_g\Delta M_g\right) = -y\frac{\Delta M_g}{M_g}. \tag{1.12}$$

If we integrate over time, imposing that all of the mass is initially in metal-free gas, we get:

$$Z_g(t) = -y\ln\left(\frac{M_g(t)}{M_g(0)}\right) = -y\ln f_g, \tag{1.13}$$

where f_g is the gas fraction (we show Z_g as a function of f_g in figure 1.1). Since Z_g and f_g are observables, it is sometimes convenient to define an *effective yield*:

$$y_{\mathit{eff}} \equiv -\frac{Z_g(t)}{\ln f_g}. \tag{1.14}$$

[8]Nuclear fusion converts some mass into energy, but the amount of mass that is converted negligible in this argument.

The Leaky Box

A number of processes can cause mass loss from a bound system, such as, winds produced by supernovae and massive stars as well as AGN. This happens for example in starburst environments where a large fraction of the gas is driven out by high mass, short lived stars. If the amount of mass that is expelled is proportional to the star formation rate, we can write:

$$\dot{M}_{\rm tot} = -\alpha \dot{M}_*. \tag{1.15}$$

Thus, at any time, $M_{\rm tot}(t) = M_{\rm tot}(0) - \alpha M_*(t)$. The implication for the gas mass is clear:

$$M_g(t) = M_{\rm tot}(t) - M_*(t) = M_{\rm tot}(0) - (1+\alpha)M_*(t). \tag{1.16}$$

We can proceed from equation 1.11 if we combine $\Delta M_* + \Delta M_g + \alpha \Delta' M_* = 0$ with the assumption that the expelled gas is of the same metallicity: $\Delta M_Z = y\Delta M_* - Z_g \Delta M_* - \alpha Z_g \Delta' M_*$.

$$\Delta Z_g = \frac{1}{M_g}\left(y\Delta M_* - Z_g \Delta M_* - \alpha Z_g \Delta' M_* - Z_g(-\Delta M_* - \alpha \Delta' M_*)\right) \tag{1.17}$$

$$\frac{dZ_g}{dM_*} = \frac{y}{M_g} = \frac{y}{M_{\rm tot}(0) - (1+\alpha)M_*(t)}. \tag{1.18}$$

Integrating this we get:

$$Z_g(t) = -\frac{y}{1+\alpha}\left\{\ln\left[M_{\rm tot}(0) - (1+\alpha)M_*(t)\right] - \ln\left[M_{\rm tot}(0) - (1+\alpha)M_*(0)\right]\right\}. \tag{1.19}$$

Assuming the initial composition is gas ($M_{\rm tot}(0) = M_g(0), M_*(0) = 0$)

$$Z_g(t) = -\frac{y}{1+\alpha}\ln\left[\frac{M_{\rm tot}(0) - (1+\alpha)M_*(t)}{M_{\rm tot}(0)}\right], \tag{1.20}$$

which can be combined with the integral form of equation 1.15 ($M_{\rm tot}(t) = M_{\rm tot}(0) - \alpha M_*(t)$):

$$Z_g(t) = -\frac{y}{1+\alpha}\ln\left[\frac{M_{\rm tot}(t) - M_*(t)}{M_{\rm tot}(0)}\right] \tag{1.21}$$

$$= -\frac{y}{1+\alpha}\ln\left[\frac{M_g(t)}{M_g(0)}\right]. \tag{1.22}$$

This reduces to equation 1.13 when $\alpha = 0$. Shown in figure 1.1 is the behaviour of the metallicity as a function of consumed/expelled gas. Note that the increase of outflow strength has a similar effect as decreasing the stellar yield.

The Accreting Box

Galaxies do not only expel mass, they build up through gas accretion. Here we neglect outflows and assume that the inflowing gas has a metallicity of 0. Since the infalling gas can either be turned into stars or left as gas, we have:

$$\Delta M_{\rm tot} = \Delta M_* + \Delta M_g. \tag{1.23}$$

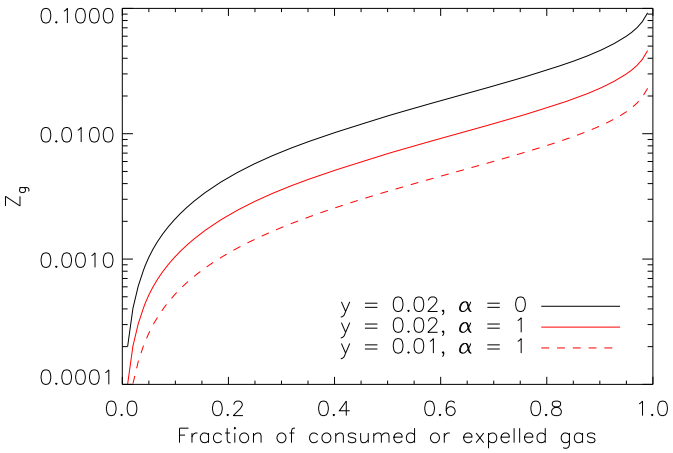

Figure 1.1: Gas Metallicity as a function of consumed/expelled gas for a closed box model (solid black), a leaky box model (solid red), and a leaky box model with a lower yield (dashed red). Note that the x axis corresponds to the stellar mass fraction for the closed box model only.

We can combine equations 1.23 and 1.10 with equation 1.11, giving:

$$\Delta Z_g = \frac{1}{M_g}\left[(y - Z_g)(\Delta M_{\rm tot} - \Delta M_g) - Z_g \Delta M_g\right], \tag{1.24}$$

$$= \frac{1}{M_g}\left[(y - Z_g)\Delta M_{\rm tot} - y\Delta M_g\right], \tag{1.25}$$

and dividing by $\Delta M_{\rm tot}$ and switching to differentials yields:

$$\frac{dZ_g}{dM_{\rm tot}} = \frac{1}{M_g}\left[y - Z_g - y\frac{dM_g}{dM_{\rm tot}}\right]. \tag{1.26}$$

If we now let $u = \int \frac{dM_{\rm tot}}{M_g}$, the above equation becomes

$$\frac{dZ_g}{du} + Z_g = y\left(1 - \frac{d\ln M_g}{du}\right), \tag{1.27}$$

whose solution is:

$$Z_g = y\left(1 - Ce^{-u} - e^{-u}\int_0^u e^{u'}\frac{d\ln M_g}{du'}\right). \tag{1.28}$$

In the case that the accretion rate plus the gas return rate is equal to the star formation rate (i.e., $\Delta M_g = 0$) we can return to equation 1.26:

$$dM_{\rm tot} = M_g\left(\frac{1}{y - Z_g}\right)dZ_g. \tag{1.29}$$

Integrating and assuming that the system is initially composed of metal-free gas ($Z_g(0) = 0$ and $M_{\rm tot}(0) = M_g(0)$):

$$\frac{M_{\rm tot}}{M_g} - 1 = \ln\frac{y}{y - Z_g}, \tag{1.30}$$

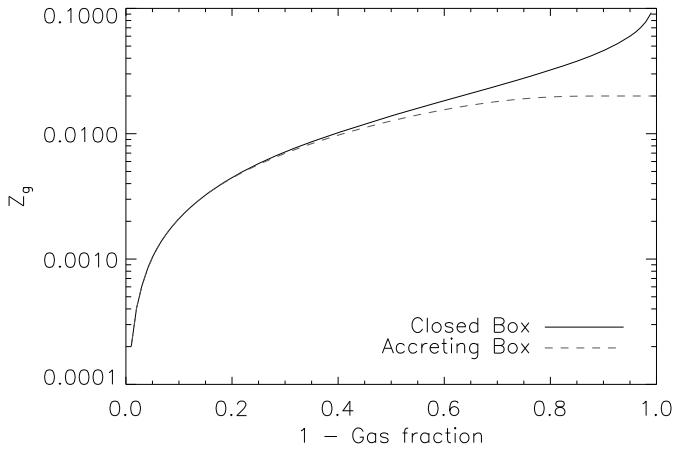

Figure 1.2: Gas Metallicity as a function of stellar fraction for a closed box model (solid black) and an accreting box model (dashed grey)

which becomes,

$$Z_g = y\left[1 - exp\left(1 - \frac{M_{\rm tot}}{M_g}\right)\right]. \tag{1.31}$$

As figure 1.2 shows, Z_g asymptotes to y for small gas fractions.

We present these models to guide the reader through the established framework in this field. We find however, the assumptions to be too restrictive, so we leave the analytic models behind while keeping in mind some of the limits and relations expressed here.

1.1.2 Numerical Calculations

If we wish to relax the instantaneous recycling approximation or consider the yields of stars of different masses/metallicities, we almost certainly need to turn to numerical methods. With a simple numerical model one can feed the chemical makeup of the recently enriched gas back into the stellar evolution of newly formed stars. Since stars of different masses lose their mass on different timescales, considering said timescales is very important when attempting to model the chemical evolution of a system.

The chemical makeup of the ejecta from a star is strongly dependent on mass. Massive stars ($M \gtrsim 8\mathrm{M}_\odot$), for instance, experience a phase of strong mass loss before ending their lives as type II (core-collapse) supernova (SNII) explosions. Such explosions occur when the energy from nuclear reactions at the star's core can no longer support the weight of the star. The outer layers collapse onto the core until electron degeneracy pressure forces the collapsing material to 'bounce' back. In general, the contributions of massive stars to cosmic pollution are mainly in the form of so-called alpha elements, such as oxygen, neon, magnesium, and silicon.

Intermediate mass stars ($0.8\ \mathrm{M}_\odot \lesssim M \lesssim 8\ \mathrm{M}_\odot$) contribute to chemical enrichment in two ways: as asymptotal giant branch (AGB) stars and type Ia supernova (SNIa). After a main sequence star has completely burned the hydrogen in its core, the star's core begins to contract while the outer layers expand as they cool. These stars are on

the red giant branch (RGB) in the Hertzsprung—Russell (HR) diagram of luminosity and temperature. When the temperature at the core of the star is high enough, helium begins to be the primary source of nuclear fusion, stalling a star's progress up the giant branch. When the helium core is exhausted, the star's envelope begins to expand again in a similar fashion to the RGB phase. The star takes a path in the HR diagram that *asymptotes* to the RGB. The instabilities resulting from hydrogen and helium burning in shells around the core, the majority of the star's mass may be lost in the AGB phase (see Herwig 2005, for an excellent review of AGB stellar evolution). This mass loss is rich in helium, carbon, and nitrogen.

Following this period of mass loss, the core (composed of mainly carbon and oxygen) of the star will be left to cool down in what is known as the white dwarf phase. During this phase, the star remains relatively inactive unless it comes into contact with another star. A merger (typically as a result of binary stellar evolution), that puts the object above the Chandrasekhar mass ($\sim 1.38\mathrm{M}_{\odot}$) will cause runaway nuclear fusion. This results because the star uses electron degeneracy pressure to support itself and does not use thermal pressure to respond to increases in temperature and therefore cannot add more pressure to counteract the heat generated from the nuclear activity. Eventually, the energy from nuclear reactions will unbind the star, resulting in what is called a type Ia supernova. The ejecta from this explosion are heavily enriched in metals, in particular iron.

Since the amount of time that stars spend on the main sequence is significant compared to the star formation timescale, it is useful to define the stellar lifetime, $\tau(M)$, as the time from stellar birth until the point at which the star leaves the main sequence. Because gravity is able to hasten the evolution of a star, its lifetime is a monotonically decreasing function of mass. The result is that high mass stars end their lives relatively quickly, while low mass stars can live for billions of years. Note that this discussion ignores the time from when a star leaves the main sequence to when it loses most of its mass (as either a SNII or an AGB star). The duration of this period is negligible with respect to the other timescales discussed here.

Type Ia supernovae, on the other hand, occur in evolved stellar systems (i.e., after one or more of the stars is already 'dead'). For SNIa, a separate rate function must be calculated since its occurrence is governed by binary as well as stellar evolution. Typically these supernovae occur over a long period of time.

Since we now have the power to follow different elements (since they are created by different processes), we must redefine the term 'yield' slightly. Recall that earlier we defined the yield y, as the metal mass ejected divided by the amount of amount of mass remaining in stars. We now use yield to refer to the elemental mass ejected from a star of a given mass and metallicity. That is, for a given stellar mass and metallicity we specify the abundance of a given element leaving the star. While this prevents us from presenting a neat analytical solution, our analysis becomes significantly more versatile.

The details of our numerical model are as follows. We begin with a reservoir of gas with arbitrary metallicity. During a given timestep $t_i + \Delta t$, we lock a certain amount of mass into stars based on a prescribed star formation rate. These stars have the metallicity of the gas out of which they formed. We then integrate the contributions from each

stellar population formed in preceding timesteps (i.e., from $t = 0$ to $t = t_i$) based on the characteristics (mass, metal content) of the stars born at that timestep. To do this, we convert time into mass using the lifetime function, then look up in yield tables the corresponding asymptotic giant branch star, supernova type II, and supernova type Ia yields. This can be written in equation form (as in chapter 3) to show the mass expelled by stars Δm_* during a single time step $(t_i, t_i + \Delta t)$ by a stellar population of initial mass $m_{*,0}$ and metallicity Z that was created at time $t_* < t_i$:

$$\Delta m_* = m_*(t_i) - m_*(t_i + \Delta t) \tag{1.32}$$

$$= m_{*,0} \int_{M_Z(t_i - t_* + \Delta t)}^{M_Z(t_i - t_*)} \Phi(M) m_{\rm ej}(M, Z)\, dM, \tag{1.33}$$

where $M_Z(\tau)$ is the inverse of the lifetime function $\tau_Z(M)$, $m_{\rm ej}(M, Z)$ is the mass ejected by a single star and $\Phi(M)$ is the stellar initial mass function (IMF), normalized such that $\int M\Phi(M)dM = 1$. It is straightforward to generalize the above equations to give $\Delta m_{*,j}$, the mass ejected in the form of element j. The functions $\tau_Z(M)$ and $m_{j,\rm ej}(M, Z)$ need to be taken from stellar evolution and nucleosynthesis calculations provided in the literature. This methodology allows us to compare yields (that is, $m_{j,\rm ej}(M, Z)$), IMFs, and type Ia supernova rates under various conditions relatively quickly.

All of the following calculations are done with our default yield set and type Ia lifetime model (Marigo 2001; Portinari et al. 1998; Thielemann et al. 2003, exponential delay function, see chapter 3). The first thing we try is to turn all of the gas into stars in one step. In that way we are simply looking at the ejecta from the stars.

In figure 1.3 we show the behaviour of this model. Notice that some elements are ejected on different timescales, corresponding to the lifetimes of the stars that produce these elements. We see that for primordial abundances, carbon, nitrogen, and iron are all produced with a delay. The former two are mainly produced by AGB stars while a significant portion of the iron comes from SNIa. These effects diminish as the initial metallicity increases since a larger fraction of the ejecta is composed of metals present at the time the star is formed. Note that here we compare to solar by using the notation $[X/{\rm H}] \equiv {\rm Log}(m_X/m_{\rm H}) - {\rm Log}(m_X/m_{\rm H})_\odot$, as is commonly done in the literature.

We next try an efolding star formation history (that is, exponentially decaying), which is similar to what is used by those who have in recent years been studying stellar populations of individual galaxies. For this calculation we have not assumed that the initial gas cloud is immediately converted into stars, as we did in the previous example. Stars are formed with a characteristic timescale of 1 Gyr (with a normalization of 1 - after 1 Gyr, $1/e$ of the gas has been turned into stars). These parameters are arbitrarily chosen to show the behaviour of such a star formation history, but this also illustrates a degree of freedom in this type of calculation. Since stars return gas to the ISM, the stellar mass fraction does not increase monotonically in this model, but peaks at approximately 40%.

In figure 1.4 we compare this model with a closed box calculation explored in the previous section (using a yield, $y = 0.02$, and the gas fraction obtained from the numerical model). The closed box model predicts the shape of the metallicity evolution well. Note that when the gas is initially not metal-free, equation 1.13 becomes:

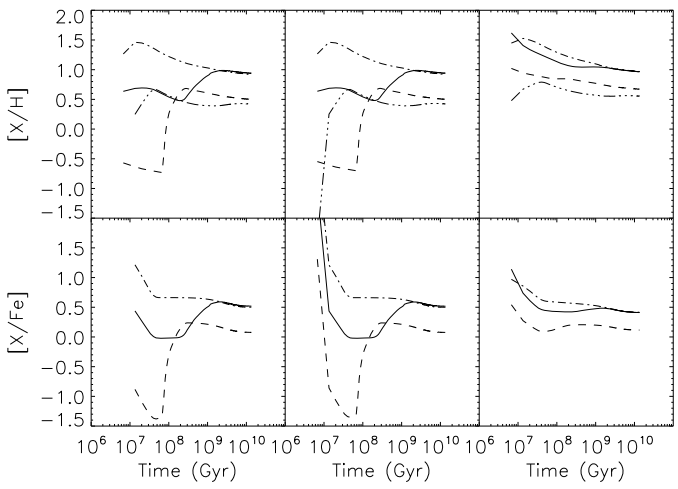

Figure 1.3: Our numerical chemical evolution model with an initial burst of star formation and a Chabrier (2003) IMF. Shown are ratios of gas abundance of element X to hydrogen (top) and iron (bottom) as a function of time. Since the burst consumes 100% of the gas, this figure effectively shows the ejecta of a single stellar population as a function of time. The left, centre, and right columns begin with primordial, 1% solar, and solar gas metallicity respectively. Elements shown are Carbon (solid), Nitrogen (dashed), Oxygen (dot-dashed) and Iron (dot-dot-dot-dashed).

$Z_g(t) = -y \ln f_g + Z_g(0)$. There is of course, a slight offset between the closed box model and the numerical result for the first time step because the closed box model assumes that the gas is instantaneously recycled while the in the numerical model there will be a delay of *at least* one time step. Many of the differences between the relative abundances seen in figure 1.3 have now disappeared since the ejecta initially make up relatively little of the gas. These differences can be seen when the abundance ratios are plotted with respect to iron, indicating that this can be an important way of evaluating chemical evolution models. We note that the final abundances do not converge to the solar values, as one might expect. It shall be seen later that uncertainties in stellar yields and SNIa rates can more than account for the difference from solar seen in figure 1.4.

Finally, we use a Strolger et al. (2004) star formation rate, which is an analytic estimation of the cosmic star formation rate. In figure 1.5 we see that with this star formation history, the initial metallicity of the gas appears to be much more important. This is only because this star formation rate results in much less stellar mass. Again, we see that the closed box model predicts the numerical solution very well. The fact that the estimates of metallicity fall below solar does not give cause for concern since this would be averaged over the entire universe and there are indeed regions of very low metallicity in the Universe at $z = 0$.

1.2 THE OWLS PROJECT

Ultimately, studying the chemical evolution of the universe is best approached using cosmological, hydrodynamical, chemodynamical simulations. Cosmological because large scales are necessary to capture the different types of objects which contribute

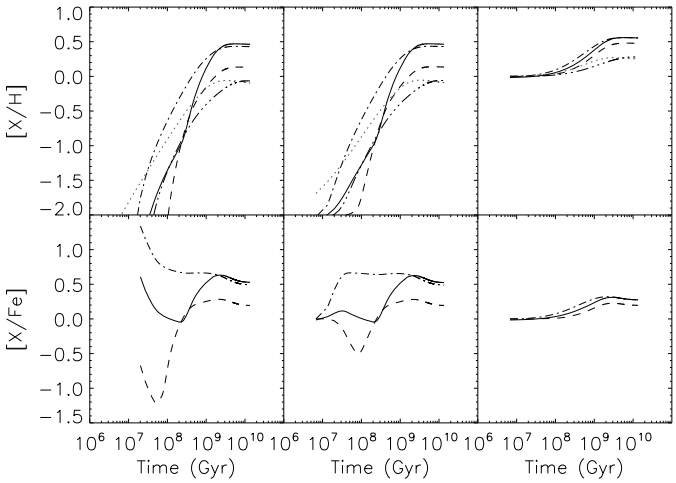

Figure 1.4: Our numerical chemical evolution model with an efolding star formation rate and a Chabrier (2003) IMF. The left, centre, and right columns begin with primordial, 1% solar, and solar gas metallicity respectively. Elements shown are Carbon (solid), Nitrogen (dashed), Oxygen (dot-dashed), and Iron (dot-dot-dot-dashed). Also shown in the top panel is the prediction from the analytical closed box model (grey dotted).

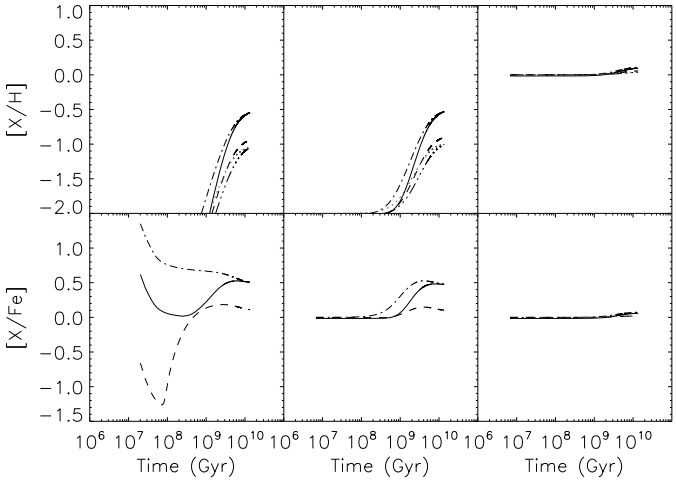

Figure 1.5: Our numerical chemical evolution model with a Strolger et al. (2004) star formation rate and a Chabrier (2003) IMF. The left, centre, and right columns begin with primordial, 1% solar, and solar gas metallicity respectively. Elements shown are Carbon (solid), Nitrogen (dashed), Oxygen (dot-dashed), and Iron (dot-dot-dot-dashed). Also shown in the top panel is the prediction from the analytical closed box model (grey dotted).

to the chemical enrichment of the universe. Hydrodynamical because gas forces play an important role in chemical evolution. Chemodynamical because it is important to follow where the produced metals originate and where they go. This method allows one to relax the instantaneous mixing approximation on large scales, as well as to investigate the chemical state of the gas in density/temperature phase space. Such an undertaking introduces new parameters that require tuning and are subject to difficulties in the interpretation of the results. Nevertheless, we will find that the chemical makeup of the IGM is complex enough that such an approach is warranted.

The idea behind the OverWhelmingly Large Simulations (OWLS) project Schaye et al. (2009) was to run a large suite of simulations, each with slightly different physical implementations or numerical parameters. Some of the aims it was conceived with are as follows:

- Quantify uncertainties due to numerical parameters.

- Quantify uncertainties due to sub-resolution physics.
- Determine which physical processes are influential in a given regime.
- Test observational/sampling biases in a controlled environment.

The process of comparing simulations with different physical models can be very instructive. It may allow us to clearly understand the physics involved in certain phenomena, or it may simply allow us determine, to first order, what is important and needs further study.

1.3 THIS THESIS

This thesis is heavily based on the OWLS project. The first half describes some of the physics that has gone into the reference model of the project, while the second half focuses more on the analysis of the simulations.

1.3.1 Chapter 2

Chapter 2 discusses how metals and a photoionizing background can effect the radiative cooling of cosmic gas. This is presented in the context of gas typical (in density, temperature, and ionizing background) of the intergalactic medium and protogalaxies. Metal enrichment typically serves to enhance cooling rates (due to the increased number of bound electrons) and photoionization typically serves to decrease cooling rates (due to the decreased number of bound electrons available and through photoheating). Although both of these effects had been previously discussed in isolation, we combine the two and explore the relative contribution of both effects for a range of densities and temperatures. We find that the density at which gas can cool in a Hubble time changes by up to an order of magnitude for given metallicity and ionization conditions. This effect occurs in a non-trivial manner, indicating self-consistent calculations are necessary for accurate cooling rates.

We demonstrate how to calculate the contributions of each element to the cooling, allowing us to relax the assumption that the relative abundances of the elements in the gas are that of solar. Even in well mixed gas, relative abundances can change by a factor of a few as it gets enriched by different processes (see the previous section). This is very important since the individual peaks of the cooling curve are very sensitive to abundances and ionization state. The cooling calculations presented in this chapter are used in the simulations presented in the rest of this thesis.

1.3.2 Chapter 3

In chapter 3 we describe the chemodynamics that goes into our simulations. We take care to consider every ingredient in turn, illustrating the uncertainties involved. The uncertainties in the stellar yields, and particularly in the supernova type Ia rates, can

amount to differences of factors of a few in metal production. We then examine the distribution of metals in the reference runs of the OWLS project, which incorporates our method. We find that simply changing the definition of the metallicity in the simulations can result in up to a factor of one and a half difference in stellar mass at $z = 0$, illustrating some of the numerical difficulties inherent to such a calculation.

The metals in our simulations are distributed relatively evenly among the cosmic gas phases at $z = 2$ and they do not follow the relative distributions of baryons, which tend to either be in a shock-heated, warm-hot phase surrounding galaxies and haloes or in a cold, diffuse phase. At $z = 0$, most of the metals are locked up in stars.

1.3.3 Chapter 4

The power of the OWLS project is finally realised in chapter 4. Here we compare the different physical models used in the various simulations in the context of the cosmic metal distribution. We examine in detail the effect of cooling, galactic wind model, stellar IMF, and feedback from AGN.

We find that strong feedback is needed to efficiently eject metals from haloes of all masses. This can come in the form of a particularly strong supernova wind model, a top-heavy IMF in high pressure regions, or feedback from AGN. In accordance with previous work, we find that the metallicity of the Warm-Hot Intergalactic Medium (WHIM) - where a large portion of the baryons in the local universe reside - to be of order $10^{-1} Z_{\odot}$, experiencing little evolution. Among all of the models this value varies by less than 0.5 dex. The only exception is the models that do not include energy feedback in the form of stellar winds and supernovae.

The metallicity of the lowest density regions - the diffuse IGM - is very sensitive the precise parameters and implementation of the feedback. This dependence can be therefore useful in gauging the validity of the different models.

We find in all models that the average stellar metallicity of the Universe is rather high ($[Z_*] \sim -1$) at high redshift ($z \sim 6$).

1.3.4 Chapter 5

The final chapter considers the origin of the $z = 0$ (that is, present day) metals. We construct an enrichment history for different gas phases at $z = 0$ in the highest resolution reference model. As expected, we find a strong density dependence, with gas of higher density being enriched later. We not only consider *when* this gas was enriched, but also by *what*. A group finder is used to determine the characteristic halo mass which enriches gas of a given density and temperature. Here too, we find a strong density gradient. Low mass haloes enrich the low density IGM while high mass haloes enrich hot gas of medium densities. This is independent of the feedback model. The cold, diffuse, underdense IGM contains very few metals, the metals that are there come mainly from intergalactic stars. The fact that much of the IGM enrichment is driven by the lowest mass haloes that we can resolve, suggests that the characteristic halo mass by which the IGM is enriched may be dependent on resolution.

1.4 Outlook

Improvement on this work will come via computer code development. Ideally we would like to be able to resolve more physics without making the simulation unfeasible, in terms of run time, data storage, or memory management. Currently run time is typically not limited by processor speed, but by communication. Since communication is not likely to improve much in the near future, better codes need to be introduced. Data storage will need to become more efficient since analysing the data is quickly becoming a computer science problem itself. Finally, if we wish to achieve higher resolutions (which may be necessary if we introduce more physics), we shall need more memory since this limits the number of particles that can be employed.

Aside from these problems, development also needs to continue for the hydrodynamical aspect of these codes. Specific to Smoothed Particle Hydrodynamics (SPH - a popular method of performing hydrodynamics calculations) it has recently become apparent that a number of 'tweaks' may need to be made to reduce numerical problems such as discreteness and lack of diffusion (e.g., Wadsley et al. 2008; Greif et al. 2009; Kawata et al. 2009). Perhaps novel approaches to hydrodynamics need to considered (e.g., Springel 2009).

New codes will hopefully also include the transfer of radiation from galactic sources throughout the IGM. While the simulations presented here assume a uniform radiation field, in reality the gas will be embedded in an inhomogeneous radiation field - particularly during reionization. This could have a large impact on the temperature structure of the IGM.

More related to the chemodynamics, the uncertainties in stellar evolution/nucleosynthesis models will hopefully be diminished in the future. Models of type Ia supernova in particular have been getting much attention as their explosion rate/mechanism is also uncertain. If we are to maintain any hope of performing any useful science with individual abundances (beyond reproducing general trends), progress in the above areas is a necessity. The uncertainties in the type Ia supernova rate in particular, result in a wide range of values for iron abundances. On the other hand these uncertainties can also be reduced observationally.

There currently exist a number of mechanisms to drive galactic winds. Such winds are thought to carry metals from the galaxies that they are produced in to the low density IGM. The only direct constraint on the nature of such winds is the energy of a supernova (assuming supernovae do indeed drive galactic winds). When attempting to account for this process in simulations, it is unclear how efficient this energy couples to the surrounding medium. At some point, a certain fraction of this energy is converted into kinetic energy as an outflow is formed. Whether this results in a large amount of mass moving at a low velocity or a small amount of mass at a fast velocity is another source of uncertainty. If one also considers other mechanisms for galactic winds (radiation pressure on dust grains, cosmic ray pressure, active galactic nucleii), then there is even more freedom available. While one may try to constrain these models indirectly with other signatures (the galactic mass-metallicity relation, IGM metallicity measurements, galactic mass functions, etc.), these tend to be degenerate with other uncertain/unresolved processes. A sound, first principles, understanding of galactic

winds is clearly necessary.

Encouragingly new instruments and telescopes will continually become available. In the next decade, a number of instruments are coming online that will be able to measure abundances for a number of temperatures and densities in the IGM. It is hoped that new X-ray instruments will finally detect and analyse the WHIM - a phase oft predicted in simulations, but not yet detected with instruments. This phase is thought to hold a good fraction of the baryons and metals in the local universe. Further measurements of abundances to greater radii in clusters will also help sort through the models. Lastly, more sensitive detectors will allow absorption lines to be measured in more and more galaxy spectra, offering a probe of the coldest portions of the IGM.

We present here a thorough treatment of the physics of the numerical models in the hope that we can understand what processes are influential so that the path ahead may become clearer.

References

Binney J., Merrifield M., 1998, Galactic astronomy. Galactic astronomy / James Binney and Michael Merrifield. Princeton, NJ : Princeton University Press, 1998. (Princeton series in astrophysics) QB857 .B522 1998 ($35.00)

Chabrier G., 2003, PASP, 115, 763

Croton D. J., Springel V., White S. D. M., De Lucia G., Frenk C. S., Gao L., Jenkins A., Kauffmann G., Navarro J. F., Yoshida N., 2006, MNRAS, 365, 11

Gnedin N. Y., Hui L., 1998, MNRAS, 296, 44

Greif T. H., Glover S. C. O., Bromm V., Klessen R. S., 2009, MNRAS, 392, 1381

Herwig F., 2005, ARA&A, 43, 435

Kauffmann G., White S. D. M., Guiderdoni B., 1993, MNRAS, 264, 201

Kawata D., Okamoto T., Cen R., Gibson B. K., 2009, ArXiv e-prints

Marigo P., 2001, A&A, 370, 194

Portinari L., Chiosi C., Bressan A., 1998, A&A, 334, 505

Schaye J., Dalla Vecchia C., Booth C. M., Wiersma R. P. C., Theuns T., Haas M. R., Bertone S., Duffy A. R., McCarthy I. G., van de Voort F., 2009, ArXiv e-prints

Shapiro P. R., Giroux M. L., Babul A., 1994, ApJ, 427, 25

Somerville R. S., Primack J. R., 1999, MNRAS, 310, 1087

Spergel D. N., Bean R., Doré O., Nolta M. R., Bennett C. L., Dunkley J., Hinshaw G., Jarosik J. L., Wollack E., Wright E. L., 2007, ApJS, 170, 377

Springel V., 2009, ArXiv e-prints

Strolger L.-G., Riess A. G., Dahlen T., Livio M., Panagia N., Challis P., Tonry J. L., Filippenko A. V., Chornock R., Ferguson H., Koekemoer A., Mobasher B., Dickinson M., 2004, ApJ, 613, 200

Sutherland R. S., Dopita M. A., 1993, ApJS, 88, 253

Talbot Jr. R. J., Arnett W. D., 1971, ApJ, 170, 409

Thielemann F.-K., Argast D., Brachwitz F., Hix W. R., Höflich P., Liebendörfer M., Martinez-Pinedo G., Mezzacappa A., Nomoto K., Panov I., 2003, in From Twilight to Highlight: The Physics of Supernovae Supernova Nucleosynthesis and Galactic Evolution. pp 331–+

Wadsley J. W., Veeravalli G., Couchman H. M. P., 2008, MNRAS, 387, 427